Communication

Nucleobase-Directed Amyloid Nanotube Assembly

Peng Liu, Rong Ni, Anil K. Mehta, W. Seth Childers, Ami Lakdawala, Sai Venkatesh Pingali, Pappannan Thiyagarajan, and David G. Lynn

J. Am. Chem. Soc., **2008**, 130 (50), 16867-16869 • DOI: 10.1021/ja807425h • Publication Date (Web): 20 November 2008

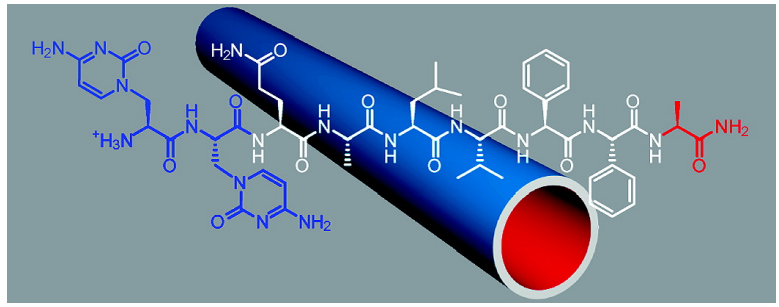

More About This Article

Additional resources and features associated with this article are available within the HTML version:

- Supporting Information
- Access to high resolution figures
- Links to articles and content related to this article
- Copyright permission to reproduce figures and/or text from this article

View the Full Text HTML

J|A|C|S
COMMUNICATIONS

Published on Web 11/20/2008

Nucleobase-Directed Amyloid Nanotube Assembly

Peng Liu,[†] Rong Ni,[†] Anil K. Mehta,[†] W. Seth Childers,[†] Ami Lakdawala,[†] Sai Venkatesh Pingali,[‡] Pappannan Thiyagarajan,[‡] and David G. Lynn*

Center for Fundamental and Applied Molecular Evolution, Departments of Chemistry and Biology, Emory University, Atlanta, Georgia 30322, and Argonne National Laboratory, Argonne, Illinois 60439

Received September 18, 2008; E-mail: david.lynn@emory.edu

The discovery of RNA as both informational template and natural catalyst questioned the strict functional division of labor implicit in the Central Dogma and gave substance to an intermediate RNA-world view of life's origins.[1,2] The structural and functional features of RNA have now been explored extensively,[3] allowing nucleic acid polymers to accurately template synthetic reactions.[4−7] The emergence of prions as epigenetic genes and templates for amyloid self-assembly[8] suggests the possibility of structurally merging RNA and protein elements to extend further the functions of each biopolymer class. Here we demonstrate incorporation of nucleic acid structural building blocks into amyloid to control morphology and create novel template scaffolds for information storage.

Amyloid assemblies, higher-order protein structures potentially accessible to all α-amino acid polymers,[9−11] are known to mediate epigenetic events in many organisms.[8] These structures contain a characteristic cross-β architecture[12,13] with orthogonal d-spacings at 0.47 and ∼1 nm arising from repeating β-strands and β-sheet laminations, respectively.[14] We extended molecular dynamics (MD) simulations[15] on amyloid to include purine and pyrimidine substitutions[16] and found that cytosine−cytosine base pairs, similar to classic i-motifs,[17,18] could be accommodated without backbone distortions (Figure 1). Previously we found[19] that Zn^{2+}-histidine

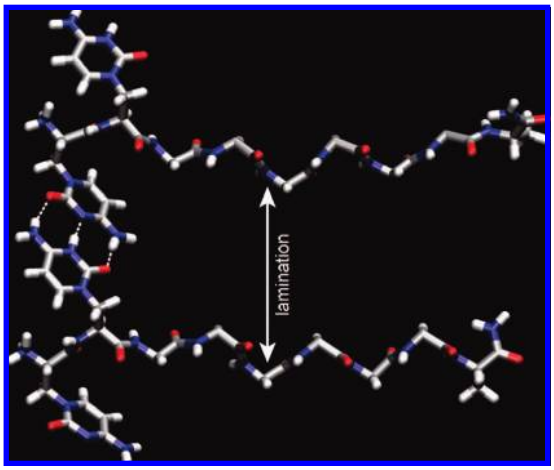

Figure 1. Proposed homocytosine base pairing with hydrogen bonds (dashed lines) developed using MD of the amyloid fibril for Aβ(13-21)cc. Only cytosine (c) side chains are shown for clarity.

coordination at the N-terminus of the Alzheimer's Disease Aβ peptide congener ^{13}HHQKLVFFA, or Aβ(13-21),[19−21] could extend β-sheet lamination and transform amyloid fibers into ribbons/tubes. Here we have replaced the N-terminal His−His dyad to test cytosine−cytosine base pairing as an innate extension of this strategy.

Accordingly, β-(cytosine-1-yl)-alanine (c)[22−26] was synthesized and substituted for H13 and H14 via solid phase synthesis within the Aβ congener to yield ccQALVFFA-NH_2, Aβ(13-21)cc (MALDI, [M + H^+] 1155.38; calcd, [M + H^+] 1154.28), where "cc" indicates the first two residues are β-(cytosine-1-yl)-alanine. HPLC purified Aβ(13-21)cc (0.3 mM) was assembled in 25 mM MES buffer across a range of pH values. Since i-motifs are comprised of hemiprotonated C−C^+ based pairs,[17,18] the pH dependent assembly of ccQALVFFA was explored. As shown in the transmission electron micrographs (TEM) in Figure 2, little assembly was

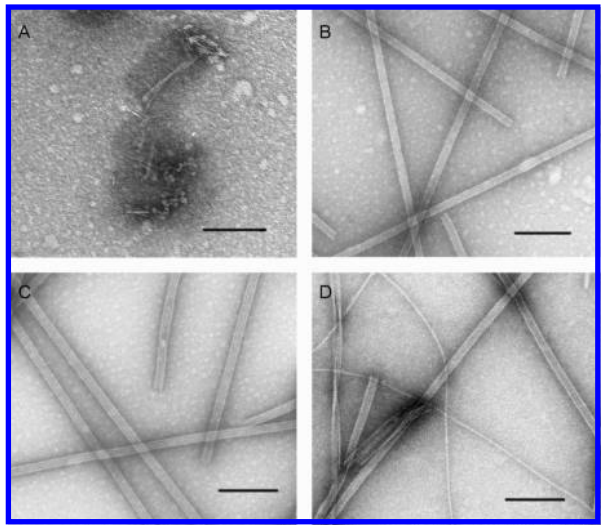

Figure 2. TEM micrographs of 0.3 mM Aβ(13-21)cc assembled in 25 mM MES buffer: A, pH = 2; B, pH = 3.3; C, pH = 4.3; D, pH = 5.5 (scale bar = 200 nm).

observed at low pH; however, at pH 3.3 and 4.3, in the range of the expected pK_a of cytosine, Aβ(13-21)cc forms large homogeneous structures that appear very similar to hollow nanotubes.[27−29] At pH 5.5, the assemblies are more heterogeneous with the appearance of ribbons and the more typical 10 nm diameter fibrils. Single cytosine substitution, Aβ(13-21)H13c or Aβ(13-21)H14c, under the same solution and pH conditions, gave only fibrils (Supporting Information, Figure S1). Together these results are consistent with the cc i-motif driving formation of hollow nanotubes.

To define the Aβ(13-21)cc nanotube architecture, small-angle X-ray scattering (SAXS) and wide-angle X-ray diffraction (XRD) experiments were performed at the 12-ID beam line at Argonne National Laboratory. Figure 3 shows a monodisperse hollow circular cylinder form factor[27] fit to the scattering data of the peptide assembly at pH 4.3 with an outer radius of 12.4 nm and a wall thickness of ∼3.3 nm.

Assignment of peptide secondary structure in the nanotube assemblies was not readily accessible by standard peptide circular

[†] Emory University.
[‡] Argonne National Laboratory.

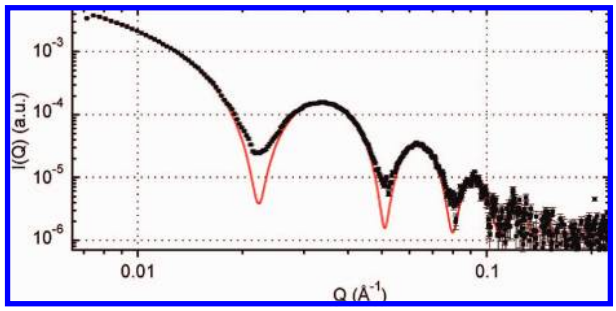

Figure 3. SAXS of 0.3 mM Aβ(13-21)cc assembled in 25 mM MES buffer at pH 4.3. Data fits to a hollow cylinder form factor (red line) with a length of 500 nm, an outer radius 12.4 ± 0.3 nm and wall thickness 3.3 ± 0.4 nm. Although the peak positions in the SAXS data are well captured by the derived parameters, the intensity remains compromised by the undetermined fraction of small aggregates contributing at these Q values.

dichroism assignments as the peptide amide electronic transitions overlapped with transitions from the cytosine bases. However, XRD of lyophilized Na_2SO_4 stabilized Aβ(13-21)cc assemblies exhibited a cross-β pattern consistent with amyloid assemblies, containing d-spacings at 4.6 and 10.3 ± 0.6 Å (Figure S2).

Cytosine stretching modes also complicated FTIR analyses, but strong amide I absorption at 1635 cm^{-1}, most consistent with parallel β-sheet rich structures, were apparent (Figure S3). Isotope-edited FTIR[30,31] with ^{13}C-labeled carbonyls incorporated at Ala16, Leu17, and Val18 exhibited amide I bands split into distinct transitions (Figure S3). The magnitude of the splitting and the band positions, which ranged from 1641 to 1638 and from 1610 to 1605 cm^{-1}, were again most consistent with a parallel in-register β-sheet orientation throughout the center of the peptide.[19]

^{13}C−^{13}C distances between ^{13}C-labeled F19 carbonyl carbons in adjacent peptides were measured using solid-state NMR double-quantum-filtered DRAWS[32,33] (DQF-DRAWS) (Figure 4a). The DQ buildup curves were fit to a three-spin model that includes the effects of measured[34] double quantum relaxation (Figure S4) and approximates an infinite array of H-bonded amide groups with ^{13}CO−^{13}CO distances of 4.6 ± 0.3 Å (Figure 4b). Therefore, the peptides form parallel in-register β-sheets, and initial studies with Ag nanoparticle binding[35] place the cytosines on the outer surface of these nanotubes.

With a 4.6 Å distance between adjacent cytosines along each β-sheet face (Figure 4c), homopyrimidine base pairing is inaccessible, but π-stacking could direct propagation along the β-sheet. As well, cc H-bonding between adjacent β-sheets may well orient the cytosine bases. Flow-oriented linear dichroism (LD) of the nanotubes evaluated the relative orientation of the $\pi-\pi^*$ peptide backbone amide (λ_{max} = 207 nm) and the cytosine in-plane (λ_{max} = 267 nm) electronic transition dipoles (Figure 5). Although some cytosine and peptide backbone amide electronic transitions overlap, the Aβ(13-21)cc positive LD signal centered at 207 nm is characteristic of the β-sheet rich amyloid fibers[36] and confirms the peptide backbone H-bonds are roughly parallel to the tube axis, as seem in the Aβ(16-22) tubes.[29] In contrast, the negative 267 nm LD transition arises only from cytosine, placing its transition dipole perpendicular to the β-sheet H-bond direction. Time-dependent DFT[37] electron structure calculations[38] indicate that the low energy 267 nm transition dipole of the hemiprotonated homocytosine base pair is ~35° away from a potential central N^{3}H−N^3 intermolecular H-bond and colinear with the long axis of each base of the homobase pair (Figure S5). These data position the cytosine bases roughly perpendicular to the tube long-axis.

Self-assembly of the β-sheet-rich amyloid structure results from many weak noncovalent interactions directing growth both along

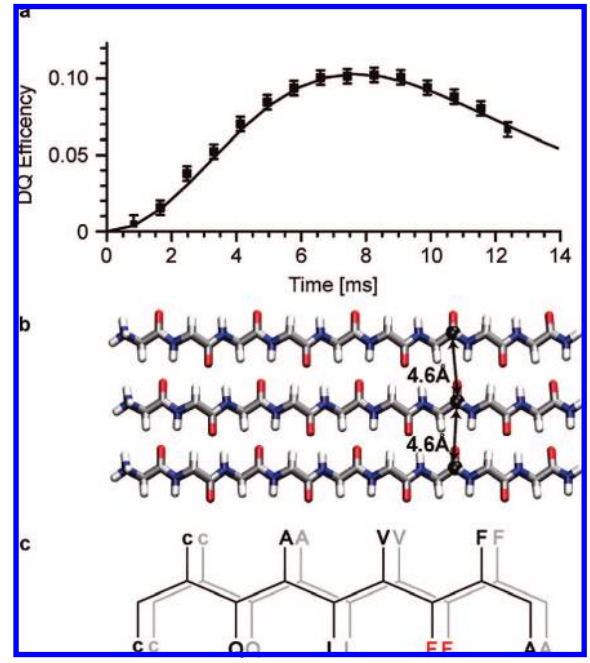

Figure 4. (a) ^{13}C DQF-DRAWS of 1 mM [1-^{13}C]F19 Aβ(13-21)cc peptide assembled in 25 mM MES buffer at pH 3.3. The solid line is the simulated DQF-DRAWS curve for an infinite array of ^{13}C−^{13}C distances of 4.6 Å with a T_{2DQ} = 9.4 ms. (b) Three in-register parallel β-strands; black spheres represent the F19 carbonyl ^{13}C. (c) Schematic β-sheet diagram showing peptide registry and residues displayed on each β-sheet face. The front peptide is colored black and ^{13}C labeled F19 residues are shaded red.

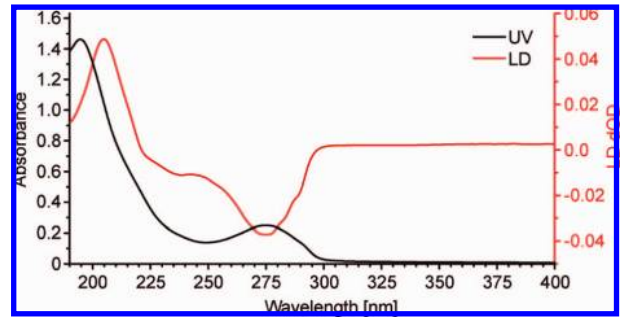

Figure 5. Ultraviolet (UV) and linear dichroism (LD) spectra of mature nanotubes assembled from 0.3 mM Aβ(13-21)cc in 25 mM MES at pH 4.3. In the UV spectrum (black), the peak at 207 nm is assigned to amide $\pi-\pi^*$ transitions and the peak at 267 nm arises from cytosine in-plane $\pi-\pi^*$ transitions. In the LD spectrum (red), the nanotubes were aligned using a Couette flow cell. The positive peak around 207 nm is consistent with the peptide amide transition dipole being more parallel to the tube axis, and the negative peak at 267 nm suggests that the cytosine transition dipole is more perpendicular to tube axis.

the β-sheets[39] and orthogonally along the sheet−sheet stacking (lamination) planes.[14] The native peptide cassette Aβ(16-22), CH_3CO-KLVFFAE-NH_2, forms nanotubes where assembly is driven by the inherent complementarity of the β-sheet faces.[14,27,29] Aβ(13-21)K16A, HHQALVFFA-NH_2,[19,21] benefits from a metal switch where Zn^{2+}−His chelation impacts nucleation, propagation, and overall laminate stability of the nanotubes. Covalent incorporation of molecular recognition elements, in this case nuclear bases, directly into the peptide framework even more profoundly impacts nanotube assembly and architecture. While amyloid fiber β-strand registry can be parallel,[40] antiparallel,[29,41] out of register[42] or even involved in folded β-sheets,[43] Aβ(13-21)cc assemblies represent the first amyloid nanotube architecture with confirmed parallel β-sheets. Moreover, the 3.3 ± 0.4 nm wall

thickness determined from SAXS establishes the wall as being a single Aβ(13-21)cc peptide thick (β-strand peptide length is 3.1 nm), significantly different from the bilayer tubes formed with other Aβ(16-22) congeners.[27,29,39] And finally, the concentration dependence for assembly is reduced by a factor of almost 10^2, underscoring the enhanced sheet–sheet association affinity.

The structure model that emerges positions the bases roughly perpendicular to parallel β-sheets, consistent with i-motif-pairing directing assembly of distinct inner- and outer-tube surfaces of a well-defined nanotube (Figure 6). Such nanotube surface asymmetry

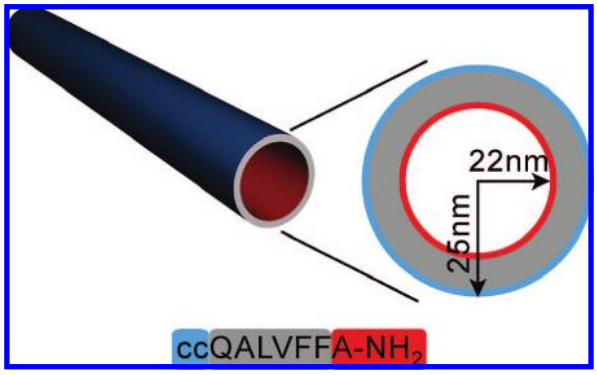

Figure 6. Schematic of the nanotube structure formed by the nucleobase-modified amyloid congener peptide. The blue/red surfaces indicate the parallel arrangement of the single-walled peptide β-sheets that result in unique inner and outer surfaces.

is not readily accessible and such archetypal assemblies highlight our ability to encode unique molecular information into amyloid assemblies for the construction of new robust nanoscale scaffolds. Of equal importance, these scaffolds extend the templates used to encode biological information beyond the nucleic acid duplexes and into covalent networks whose self-assembly depends on both precise registry and side-chain complementarity.

Acknowledgment. We thank NSF for grants CRC-CHE-0404677, CBC-CHE-0739189, and DOE ER15377 for support of these ideas and experiments, Prof. Dev Arya at Clemson University for use of LD spectropolarimeter, the Apkarian Microscopy Center of Emory University for EM analyses, and the use of IPNS and BESSRC-CAT at APS, funded by the U.S. DOE, BES under contract No. DE-AC02-06CH11357.

Supporting Information Available: Synthetic procedures and spectroscopic analyses. This material is available free of charge via the Internet at http://pubs.acs.org.

References

(1) *The RNA World*, 3rd ed.; Gesteland, R., Cech, T. R., Atkins, J. F., Eds.; Cold Spring Harbor Laboratory Press: Cold Spring Harbor, NY, 2006.
(2) Joyce, G. F.; Orgel, L. E. In *The RNA World*, 3rd ed.; Gesteland, R. F., Cech, T. R., Atkins, J. F., Eds.; Cold Spring Harbor Laboratory Press: Cold Spring Harbor, NY, 2006.
(3) Eschenmoser, A. *Science* **1999**, *284*, 2118–24.
(4) Li, X.; Zhan, Z.-Y. J.; Knipe, R.; Lynn, D. G. *J. Am. Chem. Soc.* **2002**, *124*, 746–47.
(5) Li, X.; Liu, D. R. *Angew. Chem., Int. Ed.* **2004**, *43*, 4848–70.
(6) Nielsen, P. E.; Egholm, M.; Berg, R. H.; Buchardt, O. *Science* **1991**, *254*, 1497–500.
(7) Hud, N.; Li, X.; Lynn, D. G. *Biodiversity* **2007**, *4*, 768–83.
(8) Wickner, R. B.; Edskes, H. K.; Roberts, B. T.; Baxa, U.; Pierce, M. M.; Ross, E. D.; Brachmann, A. *Genes Dev.* **2004**, *18*, 470–85.
(9) Dobson, C. M. *Nature* **2003**, *426*, 884–90.
(10) Uversky, V. N.; Fink, A. L. *Biochim. Biophys. Acta* **2004**, *1698*, 131–53.
(11) Dobson, C. M. *Methods* **2004**, *34*, 4–14.
(12) Eanes, E. D.; Glenner, G. G. *J. Histochem. Cytochem.* **1968**, *16*, 673–7.
(13) Geddes, A. J.; Parker, K. D.; Atkins, E. D. T.; Beighton, E. *J. Mol. Biol.* **1968**, *32*, 343–58.
(14) Dong, J.; Lu, K.; Lakdawala, A. S.; Mehta, A. K.; Lynn, D. G. *Amyloid* **2006**, *13*, 206–15.
(15) Lakdawala, A. S.; Morgan, D. M.; Liotta, D. C.; Lynn, D. G.; Snyder, J. P. *J. Am. Chem. Soc.* **2002**, *124*, 15150–1.
(16) Tripos International, 1699 Hanley Rd., St. Louis, MO, USA, 2007.
(17) Han, X. G.; Leroy, J. L.; Gueron, M. *J. Mol. Biol.* **1998**, *278*, 949–65.
(18) Nonin-Lecomte, S.; Leroy, J. L. *J. Mol. Biol.* **2001**, *309*, 491–506.
(19) Dong, J. J.; Shokes, J. E.; Scott, R. A.; Lynn, D. G. *J. Am. Chem. Soc.* **2006**, *128*, 3540–2.
(20) Morgan, D. M.; Dong, J. J.; Jacob, J.; Lu, K.; Apkarian, R. P.; Thiyagarajan, P.; Lynn, D. G. *J. Am. Chem. Soc.* **2002**, *124*, 12644–5.
(21) Dong, J.; Canfield, J. M.; Mehta, A. K.; Shokes, J. E.; Tian, B.; Childers, W. S.; Simmons, J. A.; Mao, Z.; Scott, R. A.; Warncke, K.; Lynn, D. G. *Proc. Natl. Acad. Sci. U.S.A.* **2007**, *104*, 13313–8.
(22) Arnold, L. D.; Kalantar, T. H.; Vederas, J. C. *J. Am. Chem. Soc.* **1985**, *107*, 7105–9.
(23) Mehta, A.; Jaouhari, R.; Benson, T. J.; Douglas, K. T. *Tetrahedron Lett.* **1992**, *33*, 5441–4.
(24) Diederichsen, U.; Weicherding, D. *Synlett.* **1999**, 917–20.
(25) Lapatsanis, L.; Milias, G.; Froussios, K.; Kolovos, M. *Synthesis* **1983**, 671–3.
(26) Dueholm, K. L.; Egholm, M.; Behrens, C.; Christensen, L.; Hansen, H. F.; Vulpius, T.; Petersen, K. H.; Berg, R. H.; Nielsen, P. E.; Buchardt, O. *J. Org. Chem.* **1994**, *59*, 5767–73.
(27) Lu, K.; Jacob, J.; Thiyagarajan, P.; Conticello, V. P.; Lynn, D. G. *J. Am. Chem. Soc.* **2003**, *125*, 6391–3.
(28) Lu, K.; Guo, L.; Mehta, A. K.; Childers, W. S.; Dublin, S. N.; Skanthakumar, S.; Conticello, V. P.; Thiyagarajan, P.; Apkarian, R. P.; Lynn, D. G. *Chem. Commun.* **2007**, 2729–31.
(29) Mehta, A. K.; Lu, K.; Childers, W. S.; Liang, Y.; Dublin, S.; Dong, J.; Snyder, J. P.; Pingali, S. V.; Thiyagarajan, P.; Lynn, D. G. *J. Am. Chem. Soc.* **2008**, *130*, 9829–35.
(30) Brauner, J. W.; Dugan, C.; Mendelsohn, R. *J. Am. Chem. Soc.* **2000**, *122*, 677–83.
(31) Paul, C.; Wang, J.; Wimley, W. C.; Hochstrasser, R. M.; Axelsen, P. H. *J. Am. Chem. Soc.* **2004**, *126*, 5843–50.
(32) Bower, P. V.; Oyler, N.; Mehta, M. A.; Long, J. R.; Stayton, P. S.; Drobny, G. P. *J. Am. Chem. Soc.* **1999**, *121*, 8373–5.
(33) Gregory, D. M.; Mehta, M. A.; Shiels, J. C.; Drobny, G. P. *J. Chem. Phys.* **1997**, *107*, 28–42.
(34) Gregory, D. M.; Benzinger, T. L.; Burkoth, T. S.; Miller-Auer, H.; Lynn, D. G.; Meredith, S. C.; Botto, R. E. *Solid State Nucl. Magn. Reson.* **1998**, *13*, 149–66.
(35) Petty, J. T.; Zheng, J.; Hud, N. V.; Dickson, R. M. *J. Am. Chem. Soc.* **2004**, *126*, 5207–12.
(36) Dafforn, T. R.; Rajendra, J.; Halsall, D. J.; Serpell, L. C.; Rodger, A. *Biophys. J.* **2004**, *86*, 404–10.
(37) Hirata, S.; Head-Gordon, M.; Bartlett, R. J. *J. Chem. Phys.* **1999**, *111*, 10774–86.
(38) Schrodinger, LLC: New York, NY, 2007.
(39) Liang, Y.; Pingali, S. V.; Jogalekar, A. S.; Snyder, J. P.; Thiyagarajan, P.; Lynn, D. G. *Biochemistry* **2008**, *47*, 10018–10026.
(40) Benzinger, T. L.; Gregory, D. M.; Burkoth, T. S.; Miller-Auer, H.; Lynn, D. G.; Botto, R. E.; Meredith, S. C. *Proc. Natl. Acad. Sci. U.S.A.* **1998**, *95*, 13407–12.
(41) Balbach, J. J.; Ishii, Y.; Antzutkin, O. N.; Leapman, R. D.; Rizzo, N. W.; Dyda, F.; Reed, J.; Tycko, R. *Biochemistry* **2000**, *39*, 13748–13759.
(42) Petkova, A. T.; Buntkowsky, G.; Dyda, F.; Leapman, R. D.; Yau, W. M.; Tycko, R. *J. Mol. Biol.* **2004**, *335*, 247–60.
(43) Petkova, A. T.; Ishii, Y.; Balbach, J. J.; Antzutkin, O. N.; Leapman, R. D.; Delaglio, F.; Tycko, R. *Proc. Natl. Acad. Sci. U.S.A.* **2002**, *99*, 16742–7.

JA807425H